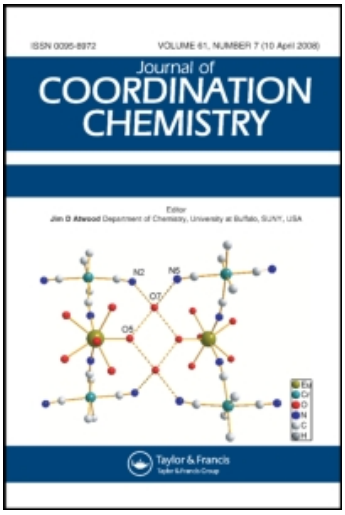

Journal of Coordination Chemistry
Publication details, including instructions for authors and subscription information:
http://www.informaworld.com/smpp/title~content=t713455674

Transition metal halide salts and complexes of 2-aminopyrimidine: manganese(II) compounds - crystal structures of (2-aminopyrimidinium)$_4$[MnCl$_4$(H$_2$O)]$_2$, [(2-aminopyrimidine)$_2$MnBr$_2$(H$_2$O)$_2$·2H$_2$O and (2-aminopyrimidinium)$^{2+}$[MnBr$_2$(H$_2$O)$_4$]Br$_2$

Jong-Ho Peter Lee[a]; Blaine D. Lewis[a]; Jessica M. Mendes[a]; Mark M. Turnbull[a]; Firas F. Awwadi[b]
[a] Carlson School of Chemistry and Biochemistry, Clark University, Worcester, MA 01610, USA [b] Department of Chemistry, Washington State University, Pullman, WA 99164, USA

Online publication date: 12 May 2010

To cite this Article Lee, Jong-Ho Peter , Lewis, Blaine D. , Mendes, Jessica M. , Turnbull, Mark M. and Awwadi, Firas F.(2003) 'Transition metal halide salts and complexes of 2-aminopyrimidine: manganese(II) compounds - crystal structures of (2-aminopyrimidinium)$_4$[MnCl$_4$(H$_2$O)]$_2$, [(2-aminopyrimidine)$_2$MnBr$_2$(H$_2$O)$_2$·2H$_2$O and (2-aminopyrimidinium)$^{2+}$[MnBr$_2$(H$_2$O)$_4$]Br$_2$', Journal of Coordination Chemistry, 56: 16, 1425 — 1442
To link to this Article: DOI: 10.1080/00958970310001642591
URL: http://dx.doi.org/10.1080/00958970310001642591

J. Coord. Chem., Vol. 56, No. 16, 10 November 2003, pp. 1425–1442

TRANSITION METAL HALIDE SALTS AND COMPLEXES OF 2-AMINOPYRIMIDINE: MANGANESE(II) COMPOUNDS – CRYSTAL STRUCTURES OF (2-AMINOPYRIMIDINIUM)$_4$ [$MnCl_4(H_2O)]_2$, [(2-AMINOPYRIMIDINE)$_2MnBr_2(H_2O)_2 \cdot 2H_2O$ AND (2-AMINOPYRIMIDINIUM)$^{2+}$[$MnBr_2(H_2O)_4$]Br_2

JONG-HO PETER LEE[a], BLAINE D. LEWIS[a], JESSICA M. MENDES[a], MARK M. TURNBULL[a,*] and FIRAS F. AWWADI[b]

[a]*Carlson School of Chemistry and Biochemistry, Clark University, Worcester, MA 01610 USA;*
[b]*Department of Chemistry, Washington State University, Pullman, WA 99164 USA*

(Received 18 April 2003; In final form 30 October 2003)

The reaction of MnX_2 (X = Cl, Br) with 2-aminopyrimidine (L) in neutral or acidic solution yields compounds of the forms $[MnCl_2L]_n$ (**1**), $(LH)_4[MnCl_4(H_2O)]_2$ (**2**), $[MnBr_2L_2(H_2O)_2] \cdot 2H_2O$ (**4**) and $(LH_2)[MnBr_2(H_2O)_4]$-Br_2 (**5**). The single-crystal X-ray structures of compounds **2**, **4**, **5** and the ligand salt, 2-aminopyrimidinium bromide, **3**, are reported. Compound **1** is proposed to form a two-dimensional coordination polymer. Compound **2** adopts a dimer structure with the Mn(II) ions bridged by two chloride ions. The dimers are linked into a ladder motif via hydrogen bonding between coordinated water molecules and adjacent chloride ions. Compound **4** is a neutral, octahedral Mn(II) complex that is linked into chains via π-stacking interactions. Compound **5** is a co-crystal of $[MnBr_2(H_2O)_4]$ and 2-aminopyrimidine dihydrobromide. Crystal data: For (**2**): monoclinic, $P2_1/c$, $a = 7.5011(15)$, $b = 16.6411(12)$, $c = 12.4462(14)$ Å; $\beta = 91.092(13)^\circ$, $V = 1533.3(4)$ Å^3, $Z = 4$, $D_{calc} = 1.740\,Mg\,m^{-3}$, $\mu = 1.541\,mm^{-1}$, $R = 0.0262$ for $[|I| \geq 2\sigma(I)]$. For (**3**): monoclinic, $P2_1/c$, $a = 4.2934(5)$, $b = 8.1959(9)$, $c = 17.439(2)$ Å; $\beta = 92.054(2)^\circ$, $V = 613.25(12)$ Å^3, $Z = 4$, $D_{calc} = 1.907\,Mg\,m^{-3}$, $\mu = 6.593\,mm^{-1}$, $R = 0.0303$ for $[|I| \geq 2\sigma(I)]$. For (**4**): triclinic, P-1, $a = 7.5312(18)$, $b = 7.7139(15)$, $c = 8.7044(14)$ Å; $\alpha = 67.482(8)^\circ$, $\beta = 84.834(13)^\circ$, $\gamma = 63.659(13)^\circ$, $V = 406.71(14)$ Å^3, $Z = 1$, $D_{calc} = 1.948\,Mg\,m^{-3}$, $\mu = 5.746\,mm^{-1}$, $R = 0.0447$ for $[|I| \geq 2\sigma(I)]$. For (**5**): orthorhombic, *Pnma*, $a = 17.1866(18)$, $b = 12.0498(12)$, $c = 7.1260(8)$ Å; $V = 1475.8(3)$ Å^3, $Z = 4$, $D_{calc} = 2.447\,Mg\,m^{-3}$, $\mu = 11.727\,mm^{-1}$, $R = 0.0550$ for $[|I| \geq 2\sigma(I)]$.

Keywords: Manganese(II); 2-Aminopyrimidine; Crystal structure; Coordination polymer

INTRODUCTION

In our study of the packing motifs of coordination complexes and salts of nitrogen heterocycles with 2+ transition metal halides, we recently examined some nickel and cobalt complexes of 2-aminopyrimidine [1] as well as copper compounds of

*Corresponding author. E-mail: Mturnbull@clarku.edu

ISSN 0095-8972 print: ISSN 1029-0389 online © 2003 Taylor & Francis Ltd
DOI: 10.1080/0095897031000164259l

2-aminopyrimidine and 2-amino-5-bromopyrimidine [2]. Common packing motifs in these compounds include bridging ligation by the pyrimidine, halide ions or both. The most common motif is the formation of hydrogen-bonded dimers of 2-aminopyrimidine or 2-aminopyrimidinium cations that leads to the formation of chains or sheets in the crystal lattice. Such influence on lattice packing has been observed in the past for various 2-aminopyrimidine and pyrimidinium complexes such as organic co-crystals of 2-aminopyrimidine with carboxylic acids [3], 2-aminopyrimidine copper(II) dicyanamides [4] and bis(2-aminopyrimidine)ethene derivatives [5]. These hydrogen-bonded dimers may be interrupted by the inclusion of waters of hydration into the lattice or by coordination of both ring-nitrogen atoms, either by metal ions or by protonation [2,6,7]. Due to the different coordination preferences of the first-row transition metals (with respect to their oxophilicity, azophilicity, etc.), different stoichiometries and coordination spheres are expected. This was observed previously with copper complexes that showed coordination of the pyrimidine ligand and no hydrates were formed [2], in contrast to cobalt complexes where both salts and neutral complexes form and the nickel complexes where both neutral complexes and hydrates are observed [1]. Here, we extend the previous work with the addition of some manganese(II) chloride and bromide complexes with 2-aminopyrimidine to see how the structure at the Mn(II) ion will affect the packing motifs.

EXPERIMENTAL

Metal salts and acids, 1-propanol and 2-aminopyrimidine were purchased from Aldrich. All materials were used as received. Infrared spectra were recorded as KBr pellets (m = medium, s = strong, br = broad, mu = multiple) on a PE-1600 or Paragon 500 infrared spectrophotometer. Magnetic susceptibility measurements were made on a Johnson-Matthey susceptibility balance at room temperature (~23°C). No attempts were made to maximize yields from crystallizations.

*μ-2-Aminopyrimidine-μ-dichloromanganese(II) (**1**)* Method A: A solution of 2-aminopyrimidine (1.90 g, 20 mmol) and $MnCl_2 \cdot 4H_2O$ (3.964 g, 20 mmol) in water (20 mL) was left overnight at room temperature. Traces of a brown powder (presumably MnO_2) were filtered off and the resulting pale yellow solution was reduced under a slow stream of N_2 over two days. The resulting pale pink crystals were recovered by filtration and air-dried to give 0.581 g (13%). Method B: 2-Aminopyrimidine (0.995 g, 10 mmol) was dissolved in hot 1-propanol (5 mL) and added to a hot solution of $MnCl_2 \cdot 4H_2O$ (1.982 g, 10 mmol) in 1-propanol (12 mL). A light pink precipitate formed immediately. The mixture was then allowed to cool, filtered and the so-obtained precipitate washed with cold 1-propanol. The solid was left to air-dry and gave 0.574 g (26%). IR (cm^{-1}): 3450m br, 1642s, 1572s, 1497s, 1361s, 1328m, 1198m, 815m, 793s, 660s, 513m, 475m. $\chi_g = 7.26 \times 10^{-5}$ cgs. Anal. Calcd. (%) for $C_4H_5N_5Cl_2Mn$: C, 21.72; H, 2.26; N, 19.00. Found: C, 21.96; H, 2.41; N, 18.78.

*Tetrakis(2-aminopyrimidinium) bis[tetrachloroaquamanganese(II)] (**2**)* $MnCl_2 \cdot 4H_2O$ (1.98 g, 10 mmol) was dissolved in H_2O (5 mL) and added to a solution of 2-aminopyrimidine (1.88 g, 20 mmol) and HCl (conc., 1.7 mL, 20 mmol) in H_2O (5 mL). The resulting colorless solution was left to evaporate at room temperature. After one month pale pink blocks of **2** were collected and air-dried to give 3.58 g (88%).

Mp = 204–205°C. IR ν (cm^{-1}): 3310s br, 1672s, 1656s, 1622s, 1539w, 1348m, 1288w, 1211w, 1072w, 993w, 792w, 778m, 530m. $\chi_g = 4.01 \times 10^{-5}$ cgs.

*2-Aminopyrimidinium bromide (**3**)* Compound **3** was isolated as the principal product from the reaction of $MnBr_2$ with one equivalent of 2-aminopyrimidine and HBr in aqueous solution. A solution of 2-aminopyrimidine (1.90 g, 20 mmol) in 1.0M HBr (20 mL) was added to a solution of $MnBr_2$ (4.295 g, 20 mmol) in water (10 mL). The solution was filtered to remove traces of brown solid (presumably MnO_2) and then concentrated by warming on a hot plate. The initial precipitate (1.52 g) was isolated and characterized as $MnBr_2 \cdot 4H_2O$ by IR and magnetic susceptibility. Further evaporation of the filtrate at room temperature gave rod-shaped crystals of **3** (0.975 g, 15.7%) and a small amount of cubic crystals that were removed by hand under a stereomicroscope (IR and χ_g showed these crystals to be **4**, below). Mp = 143–144°C. IR ν (cm^{-1}): 3347m, 3196m, 3144m, 2661m br, 1670s, 1638s, 1618s, 1538m, 1344s, 992m, 864m, 793m, 613m br, 506m.

*bis(2-Aminopyrimidine)diaquadibromomanganese(II) dihydrate (**4**)* 2-Aminopyrimidine (3.80 g, 40 mmol) was dissolved in 1M HBr (40 mL) and added to a solution of $MnBr_2$ (4.295 g, 20 mmol) in water (10 mL). The solution was warmed and the resulting white precipitate (hydrated $MnBr_2$) was filtered off. The filtrate was left to evaporate at room temperature and produced small cube-shaped crystals that were isolated by filtration and air-dried to give 0.75 g (11%) of **4**. Mp = 280°C d. IR ν (cm^{-1}): 3500–2800m br, 3410s, 3315s, 1620s, 1572s, 1486s, 1358m, 1223w, 1191m, 795m, 658m, 462m. $\chi_g = 3.11 \times 10^{-5}$ cgs.

*2-Aminopyrimidinium(2+) tetraaquadibromomanganese(II) dibromide (**5**)* 2-Aminopyrimidine (1.90 g, 20 mmol) was dissolved in 5.5M HBr (20 mL). $MnBr_2$ (2.147 g, 10 mmol) was dissolved in water (3 mL) and the resulting turbid mixture filtered to remove traces of MnO_2. The solutions were combined and then left under a slow stream of N_2 until crystals began to form. A crystal was removed from the mixture; the mixture was then warmed until a solution was attained. The resulting orange solution was allowed to cool to room temperature, seeded with the retained crystal and left to crystallize. Cube-shaped crystals were recovered by filtration and air-dried to give X-ray quality crystals of **5** (0.592 g; 11%). Additional crystals formed in the filtrate gave an additional 0.94 g (17%) that proved to be the same material by IR. Mp = 245–250°C d. IR ν (cm^{-1}): 3388s, 3302s, 3226s, 3095s, 2681m br, 1702s, 1620s, 1405m, 1282m, 1209m, 775m, 639m. $\chi_g = 2.69 \times 10^{-5}$ cgs.

X-ray Structure Determination

Data collections for **2**, **4**, **5** were carried out on a Siemens $P2_1$ diffractometer upgraded to P4 employing MoKα radiation ($\lambda = 0.71073$ Å) and a graphite monochromator. Data collection via ω-scans and cell refinement were performed using Bruker XSCANS software [8] and data reduction was performed using Bruker SHELXTL software [9]. Absorption corrections were made via ψ-scans. Data collection for **3** was carried out on a Bruker/Siemens SMART APEX system employing MoKα radiation ($\lambda = 0.71073$ Å) and a graphite monochromator. Data collection via ω-scans using Bruker SMART software and cell refinement and data reduction was performed using Bruker SAINT software [10]. Absorption corrections were made via SADABS [11]. All structures were solved using the heavy atom Patterson method [SHELXS-97] and

full-matrix least-squares refinement was done via SHELXL-97 [12]. The aromatic hydrogen atoms were refined via a riding model with fixed isotropic *U*s except for **2** where the coordinates were refined. The coordinates of the NH and OH hydrogens were located in the difference maps and allowed to refine with fixed isotropic *U*s. For **5**, the O–H bond lengths were fixed at 1.00(2) Å as attempts to freely refine the coordinates resulted in unacceptably short bond lengths. This resulted in a short interatomic distance for H2···H2B. Crystallographic data (Table I), selected bond lengths and angles (Table II) and hydrogen bonds (Table III) are given here. Full crystallographic details, atomic coordinates and isotropic thermal parameters, full tables of bond lengths and angles, observed and calculated structure factors and anisotropic thermal parameters are available [13].

TABLE I Crystal data and structure refinement for **2**–**5**

	2	*3*	*4*	*5*
Empirical formula	$C_8H_{14}N_6OCl_4Mn$	$C_4H_6N_3Br$	$C_8H_{18}N_6O_4MnBr_2$	$C_4H_{15}N_3O_4MnBr_4$
Formula weight	406.99	176.03	477.04	543.77
Crystal system	monoclinic	monoclinic	triclinic	orthorhombic
Crystal habit	irr. chunk	rod	rect. prism	prism
Space group	$P2_1/c$	$P2_1/c$	*P*-1	*Pnma*
Unit cell dimensions				
a (Å)	7.5011(15)	4.2934(5)	7.3512(18)	17.1866(18)
b (Å)	16.6411(12)	8.1959(9)	7.7139(15)	12.0498(12)
c (Å)	12.4462(14)	17.439(2)	8.7044(14)	7.1260(8)
α (°)	90	90	67.482(8)	90
β (°)	91.092(13)	92.054(2)	84.834(13)	90
γ (°)	90	90	63.659(13)	90
Volume (Å^3)	1553.3(4)	613.25(12)	406.71(14)	1475.8(3)
Z	4	4	1	4
D_c (g cm^{-3})	1.740	1.907	1.948	2.447
Size (mm)	0.15 × 0.3 × 0.2	0.23 × 0.05 × 0.05	0.08 × 0.15 × 0.08	0.2 × 0.4 × 0.35
F(000)	820	344	235	1028
μ (mm^{-1})	1.541	6.593	5.746	11.727
Data collection				
T (K)	295(2)	81(2)	295(2)	295(2)
Max., min. transmission	0.6014–0.5361	0.7340–0.3124	0.8597–0.6858	0.9419–0.3172
Reflections collected	3663	7497	1743	1875
Independent reflections	2740	1720	1390	1370
θ range (°)	2.04–25.00	2.34–30.03	2.54–25.0	2.37–25.0
Range h, k, l	$1 \le h \le 8$	$-6 \le h \le 6$	$-8 \le h \le 1$	$-1 \le h \le 20$
	$-19 \le k \le 1$	$-11 \le k \le 11$	$-8 \le k \le 7$	$-14 \le k \le 1$
	$-14 \le l \le 14$	$-23 \le l \le 24$	$-10 \le l \le 10$	$-8 \le l \le 1$
Refinement				
Extinction coeff.	0.0105(10)	none	none	0.0108(10)
Data/restraints/para.	2740/0/224	1720/0/82	1390/0/115	1370/4/101
Goodness-of-fit on F^2	1.020	1.062	1.031	1.039
Final R indices [$I > 2\sigma(I)$]				
R_1	0.0262	0.0303	0.0447	0.0550
wR_2	0.0623	0.0677	0.0916	0.1297
R indices (all data)				
R_1	0.0348	0.0391	0.0690	0.0924
wR_2	0.0661	0.0708	0.1014	0.1539
Largest diff. peak (e Å^{-3})	0.249	1.204 (near Br1)	0.565	1.070 (near Br2)
Largest diff. hole (e Å^{-3})	−0.260	−0.675	−0.826	−0.880

TABLE II Selected bond lengths (Å) and angles (°) for **2**–**5**

		2		*4*		*5*	
M–X1	Mn–Cl1	2.5879(6)	Mn–Br1	2.7108(8)	Mn–Br1	2.655(2)
M–X2	Mn–Cl2	2.5130(6)					
M–X3	Mn–Cl3	2.5167(7)					
M–X4	Mn–Cl4	2.4972(8)					
M–X5	Mn–Cl1#1	2.5535(6)					
M–N or O	Mn–O1	2.2597(16)	Mn–N1	2.335(5)	Mn–O1	2.193(8)
			Mn–O1	2.154(5)	Mn–O2	2.210(9)
					Mn–O3	2.196(8)
X1–M–X2	Cl1–Mn–Cl2	89.623(19)			Br1–Mn–Br1#2	91.22(9)
X1–M–X3	Cl1–Mn–Cl3	174.83(2)				
X1–M–X4	Cl1–Mn–Cl4	90.90(2)				
X1–M–X5	Cl1–Mn–Cl1#1	85.796(19)				
X1–M–N1/O1	Cl1–Mn–O1	87.41(5)	Br1–Mn–O1	88.14(13)	Br1–Mn–O1	90.3(2)
			Br1–Mn–N1	88.33(12)	Br1–Mn–O2	93.3(2)
					Br1–Mn–O3	93.5(2)
X2–M–X3	Cl2–Mn–Cl3	95.37(2)				
X2–M–X4	Cl2–Mn–Cl4	99.70(2)				
X2–M–X5	Cl2–Mn–Cl1#1	168.07(2)				
X2–M–N or O	Cl2–Mn–O1	81.48(5)				
X3–M–X4	Cl3–Mn–Cl4	89.56(2)				
X3–M–X5	Cl3–Mn–Cl1#1	89.05(2)				
X3–M–N or O	Cl3–Mn–O1	92.02(5)				
X4–M–X5	Cl4–Mn–Cl1#1	91.39(2)				
X4–M–N or O	Cl4–Mn–O1	177.94(5)				
X5–M–N or O	Cl1#1–Mn–O1	87.30(5)				
O–M–O or N			N1–Mn–O1	89.08(18)	O1–Mn–O2	86.1(3)
O1–M–O3					O1–Mn–O3	86.9(3)
O2–M–O3					O1–Mn–O1#2	88.2(5)
O3–M–O3					O2–Mn–O3	170.2(4)
	Mn#1–Cl(1)–Mn	94.204(19)				

Symmetry operations: #1: $-x+1,-y+1,-z+1$; #2: x, $-y+1/2$, z.

RESULTS AND DISCUSSION

Synthesis

Reaction of 2-aminopyrimidine (2-apm) with $MnCl_2$ in a 1 : 1 or 2 : 1 ratio in water or 1-propanol gave $[MnCl_2(2\text{-apm})]$ (**1**) as pale pink crystals.

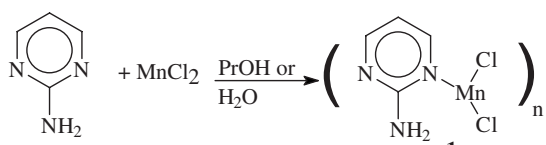

Two equivalents of 2-apm reacted with $MnCl_2$ in dilute aqueous HCl to give the dimeric manganese complex $(2\text{-apmH})_4[MnCl_4(H_2O)]_2$ (**2**) also as pale pink crystals.

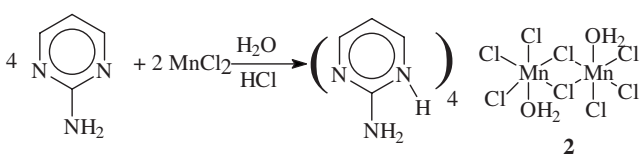

TABLE III Hydrogen bonds for **2**–**5** [Å and °]

For compound **2**

D–*H*···*A*	*d*(*D*–*H*)	*d*(*H*···*A*)	*d*(*D*···*A*)	∠(*DHA*)
O(1)–H(1A)···N(11)	0.81(3)	2.13(3)	2.925(3)	167(3)
O(1)–H(1B)···Cl(4)#2	0.82(3)	2.44(3)	3.1194(18)	141(2)
N(2)–H(2B)···Cl(2)#3	0.85(3)	2.57(3)	3.355(3)	153(3)
N(3)–H(3)···Cl(4)#4	0.77(3)	2.35(3)	3.071(2)	156(3)
N(12)–H(12A)···Cl(2)#5	0.88(3)	2.40(3)	3.207(2)	152(2)
N(12)–H(12B)···Cl(3)	0.82(3)	2.36(3)	3.159(2)	169(3)
N(13)–H(13)···O(1)#5	0.77(3)	2.17(3)	2.910(2)	162(3)

Symmetry operations used to generate equivalent atoms:
#1 $-x+1, -y+1, -z+1$; #2 $x+1, y, z$; #3 $x-1, -y+3/2, z-1/2$; #4 $-x, -y+1, -z$; #5 $x, -y+3/2, z-1/2$.

For compound **3**

D–*H*···*A*	*d*(*D*–*H*)	*D*(*H*···*A*)	*d*(*D*···*A*)	∠(*DHA*)
N(1)–H(1)···Br(1)#1	0.83(3)	2.39(3)	3.197(2)	163(3)
N(2)–H(2A)···Br(1)	0.93(3)	2.49(3)	3.397(2)	164(3)
N(2)–H(2B)···N(3)#1	0.83(3)	2.45(3)	3.031(3)	128(3)
N(2)–H(2B)···Br(1)#1	0.83(3)	2.92(3)	3.576(2)	137(3)

Symmetry operations used to generate equivalent atoms: #1 $-x, y-1/2, -z+1/2$.

For compound **4**

D–*H*···*A*	*d*(*D*-*H*)	*d*(*H*···*A*)	*d*(*D*···*A*)	∠(*DHA*)
O(1)–H(1A)···O(2)#2	0.86(7)	1.92(7)	2.734(7)	157(6)
O(1)–H(1B)···O(2)#3	0.74(7)	2.02(7)	2.743(7)	164(8)
N(2)–H(2A)···Br(1)#1	0.91(7)	2.60(8)	3.427(6)	151(6)
N(2)–H(2A)···O(1)	0.91(7)	2.64(7)	3.089(7)	112(5)
N(2)–H(2B)···Br(1)#4	0.76(8)	2.80(8)	3.556(6)	170(8)
O(2)–H(3A)···N(3)#5	0.80(8)	1.98(8)	2.770(7)	169(8)
O(2)–H(3B)···Br(1)	0.74(8)	2.69(8)	3.382(5)	156(8)

Symmetry operations used to generate equivalent atoms:
#1 $-x, -y+2, -z+2$; #2 $x, y+1, z$; #3 $-x+1, -y+1, -z+2$; #4 $x, y, z+1$; #5 $x, y, z-1$.

For compound **5**

D–*H*···*A*	*d*(*D*–*H*)	*d*(*H*···*A*)	*d*(*D*···*A*)	∠(*DHA*)
O(3)–H(3)···Br(2)#3	0.98(2)	2.45(5)	3.315(6)	146(7)
O(2)–H(2)···Br(2)	1.00(2)	2.34(3)	3.305(7)	163(8)
O(1)–H(1B)···Br(2)#4	1.00(2)	2.49(4)	3.459(8)	162(9)
O(1)–H(1A)···Br(1)#5	1.00(2)	2.37(5)	3.300(8)	155(9)
N(1)–H(1)···Br(2)#1	1.17(10)	2.07(10)	3.198(8)	161(8)
N(2)–H(2A)···Br(1)#6	0.93(11)	2.81(11)	3.406(12)	123(9)

Note: O–H bonds in **5** were restrained to 1.00(2) Å. Symmetry operations used to generate equivalent atoms:
#1 $x, -y+1/2, z$; #2 $x, -y+3/2, z$; #3 $x+1/2, y, -z+1/2$; #4 $-x, -y, -z$; #5 $-x+1/2, -y, z-1/2$;
#6 $-x, -y+1, -z+1$.

Attempts to prepare related compounds from $MnBr_2$ in dilute aqueous HBr resulted in the isolation of the ligand salt, 2-apmHBr, **3**, as colorless rods. At higher relative concentrations of 2-apm in either neutral solution or dilute aqueous HBr the neutral complex $[MnBr_2(2\text{-apm})_2(H_2O)_2]$ was isolated as the dihydrate **4**. Repeated attempts to prepare the 1 : 1 complex were unsuccessful.

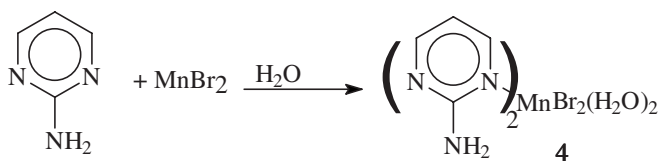

4

In an attempt to prepare $MnBr_2$ complexes containing the 2-aminopyrimidinium ion, the synthesis was repeated in 5.5 M HBr, which resulted in the isolation of 2-aminopyrimidinium(2+)$Br_2 \cdot MnBr_2(H_2O)_4$ (**5**).

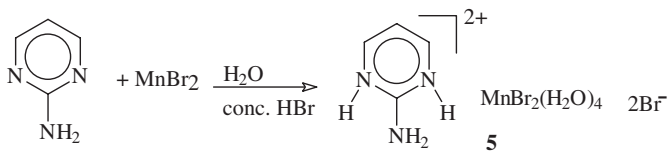

The complexes were analyzed by IR, room temperature magnetic susceptibility and single crystal X-ray diffraction. Crystallographic data for **2**–**5** (Table I) and selected bond lengths and angles (Table II) are given here. Repeated attempts from several solvent systems failed to produce suitable crystals of **1**.

X-ray Structures

The manganese complex **2** crystallizes as (2-apmH) cations and chloride bi-bridged $Mn_2(H_2O)_2Cl_8$ dimers (Fig. 1). The water molecules occupy *trans* axial positions within the dimeric unit.

The coordination sphere about the manganese ions in the $[Mn(H_2O)Cl_4]_2$ units is distorted octahedral. The largest deviations from idealized bond angles involve Cl2 [$\angle_{Cl2-Mn-Cl4} = 99.70(2)^\circ$; $\angle_{Cl4-Mn-O} = 81.48(5)^\circ$]. The Mn–Cl bond lengths are all similar, with the bonds to the bridging chlorines being lengthened by less than 0.1 Å [range: 2.4972(8) Å (Mn–Cl4) to 2.5879(6) Å (Mn–Cl1)]. The Mn–Cl1–MnA–Cl1A central unit (Fig. 1) is planar, as required by symmetry with the angle at the Mn equal to 85.80(2)° and at the bridging Cl atoms equal to 94.20(2)°. Bond lengths and angles

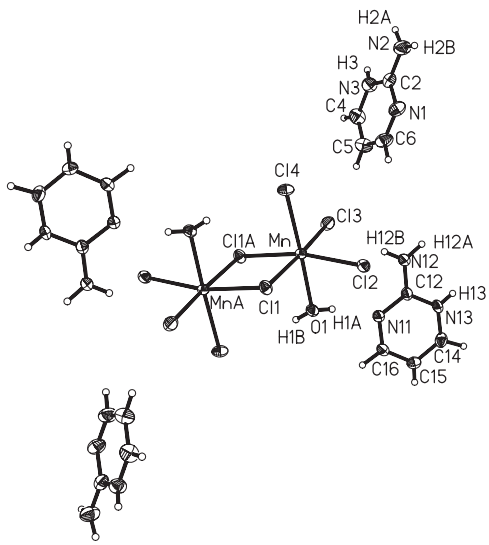

FIGURE 1 Thermal ellipsoid diagram of the dimeric unit of **2**. Only the asymmetric unit, Mn coordination sphere and hydrogens whose positions were refined are labeled. Hydrogen atoms are shown as circles of arbitrary size.

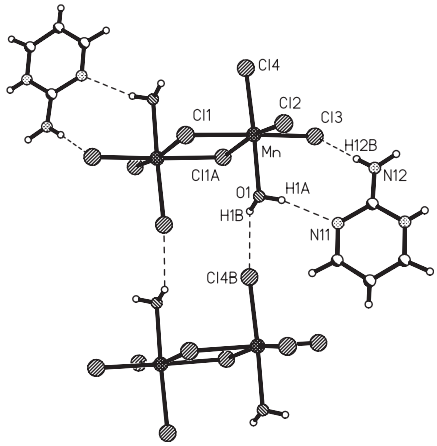

FIGURE 2 Packing of **2**, showing the ladder motif for the Mn(II) dimers. Dashed lines show hydrogen bonds.

within the two independent pyrimidine rings are similar, with the greatest differences seen in the N1–C2 and N11–C12 bond lengths [1.343(3) and 1.356(3) Å, respectively] and the C6–N1–C2/C16–N11–C12 bond angles [116.9(2) and 121.6(3)°, respectively]. This difference most likely results from the difference in hydrogen bonding between the two rings as N11 serves as an H-bond acceptor, while N1 does not.

The packing of the $[Mn(H_2O)Cl_4]_2$ units shows a ladder motif (Fig. 2). The rungs of the ladder are formed by the Mn_2Cl_2 links. The dimers are then stacked parallel to the *a*-axis with successive dimers related by a unit cell translation to form the ladder rails. The ladders are stabilized by hydrogen bonding between the water molecules and chloride ions of adjacent dimers [$d_{O1–H1B\cdots Cl4B} = 3.119(2)$ Å, $\angle_{O1–H1B\cdots Cl4B} = 141(2)°$; symm. operation $Cl4B = x+1, y, z$]. Using Etter's notation [14] the hydrogen bonding which forms the ladders is an $R_2^2(12)$ system, indicating ring formation with two hydrogen bond donors and two hydrogen bond acceptors forming a twelve-membered ring. Several additional hydrogen bonds are present in the lattice (Figs. 2 and 3, Table III), the strongest of which occur between the water molecule and N11 [$d_{O1–H1A\cdots N11} = 2.925(3)$ Å, $\angle_{O1–H1A\cdots N11} = 167(3)°$] and between N13 and the water oxygen [$d_{N13–H13\cdots O1A} = 2.910(2)$ Å, $\angle_{N13–H13\cdots O1A} = 162(3)°$; symm. operation $O1A = x, -y+3/2, z-1/2$]. These result in two additional hydrogen-bonding motifs between the N11 pyrimidine ring and the dimer [$N_1 = R_2^2(8)\,R_2^2(8)$; $N_2 = R_4^4(14)$] that link the ladders into a three-dimensional network.

The 2-apmH cations occupy channels formed between the Mn ladders, isolating the ladders from each other (Fig. 3).

Within the channels, the 2-apmH ions are found as truncated stacks containing four cations running parallel to the (011) direction (Fig. 4). This π–π stacking is extremely efficient, with interplanar distances of 3.349 Å for ring N1–ring N11 and 3.489 Å for ring N1–ring N1A* (symm. transformation $= 1-x, -y, -z$).

The rings are nearly parallel with angles between their mean planes of 4.6(2)° (N1–N11) and 0° (N1–N1A, as required by symmetry). The distances between the ring centers are 3.847(3) Å (N1–N11) and 3.688 Å (N1–N1A) and the angles between the lines connecting those centers and the mean ring planes are 28.2(3)° and 16.2(3)°, respectively.

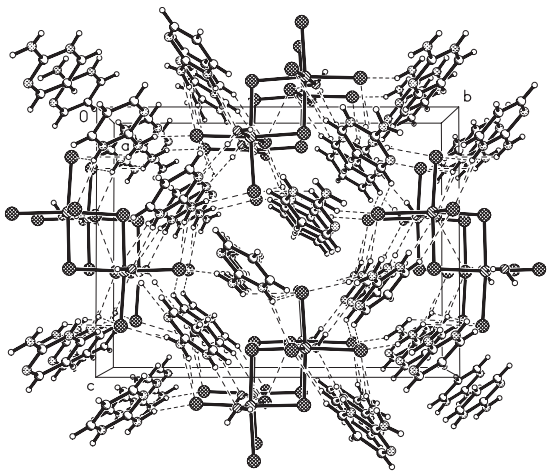

FIGURE 3 Packing diagram of **2** viewed parallel to the *a*-axis, showing the isolation of the Mn ladder motifs by the organic cations.

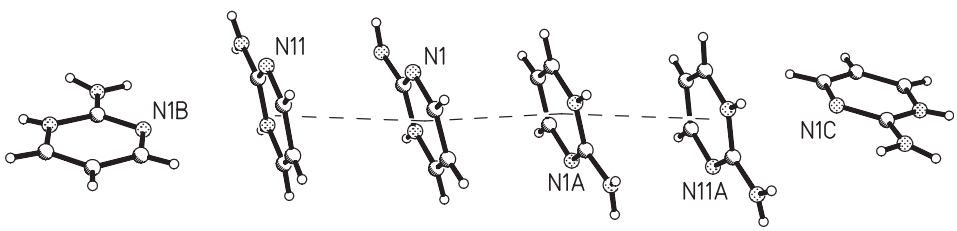

FIGURE 4 Truncated π–π stacks in **2**.

Compound **3** was isolated as a by-product of attempts to synthesize $MnBr_2$ complexes in dilute aqueous HBr. The asymmetric unit is shown in Fig. 5. Bond lengths within the ring agree with the corresponding bonds in **2** within ± 0.01 Å. Bond angles are also similar (with $\pm 1^\circ$) except at the unprotonated ring-nitrogen where $\angle$C2–N3–C4 = 116.8(2)°, matching only the corresponding angle in the N1-ring of **2**, an apparent result of the different H-bonding observed (see below).

The packing of compound **3** is controlled by a combination of hydrogen bonds and stacking interactions (Fig. 6). The strongest H-bond is observed between N1 and Br1 [$d_{N1–H1\cdots Br1A} = 3.197(2)$ Å, $\angle_{N1–H1\cdots Br1A} = 163(3)^\circ$; symm. operation for Br1A = $-x$, $y - 1/2$, $-z + 1/2$]. A bifurcated hydrogen bond between N2–H2B and N3 [$d_{N2–H2B\cdots N3A} = 3.031(3)$ Å, $\angle_{N2–H2B\cdots N3A} = 128(3)^\circ$; symm. operation for N3A = $-x$, $y - 1/2$, $-z + 1/2$], and N2–H2B and Br1 [$d_{N2–H2B\cdots Br1A} = 3.576(2)$ Å, $\angle_{N2–H2B\cdots Br1A} = 137(3)^\circ$] is also present. The combination of these generates two rings [$N_1 = R_2^3(6)$ $R_2^1(6)$] that link the system into an extended chain network [$N_2 = C(6)$ C(4)]. Stacking interactions between the 2-aminopyrimidine rings generate chains (Fig. 7). The rings stack such that the amino group of one ring lies nearly directly under the next ring in the chain. The distance between the N2 atom and the ring centroid is 3.312(2) Å and the angle between that line and the normal to the mean ring plane is 4.9(2)°.

The neutral compound **4** crystallized from dilute HBr_{aq} with two coordinated water molecules and two additional lattice water molecules (Fig. 8). The coordination sphere

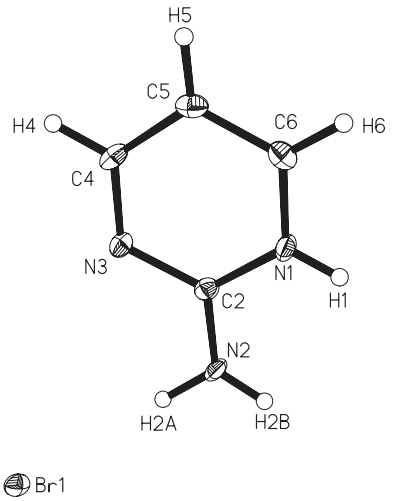

FIGURE 5 Thermal ellipsoid diagram of **3**. Hydrogen atoms are shown as arbitrary spheres.

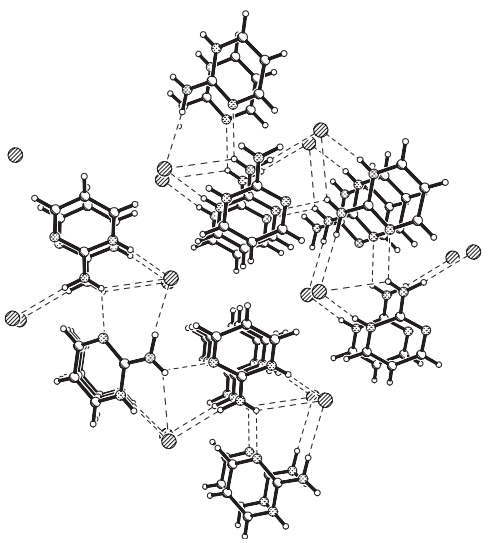

FIGURE 6 Packing diagram of **3** viewed parallel to the *a*-axis, showing hydrogen bonds as dashed lines.

is quite regular with the Mn ion located on an inversion center. The largest deviation in angle is Br1–Mn–O1 [88.14(13)°]. The closest related complex is the bis[2,3,5,6-tetrafluro-1,4-bis(4-pyridylsulfenyl)benzene]bis(ethanol)$MnBr_2$ complex [15], which also contains the neutral $MnBr_2O_2N_2$ core. The Mn–Br bond in **4** is slightly longer [2.7108(8) *vs* 2.677(3) Å], as is the Mn–N bond [2.335(5) *vs* 2.317(13) Å] while the Mn–O bond in **4** is somewhat shorter [2.154(5) *vs* 2.216(12) Å].

Bond lengths within the pyrimidine ring are comparable to those seen in **2** and **3**. Most angles within the ring are equivalent (±1°), although the C12–N13–C14 bond angle is smaller than the corresponding angle in **2** and **3** by ~5° and the

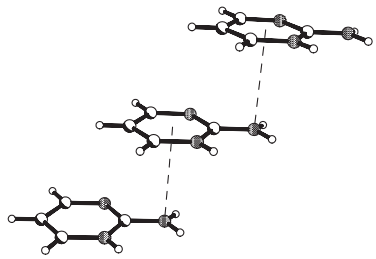

FIGURE 7 Stacking interactions in **3**.

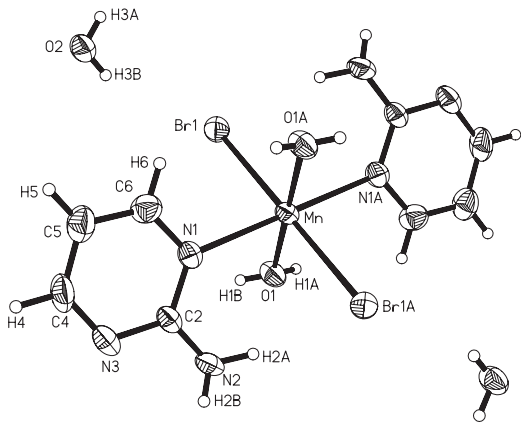

FIGURE 8 Thermal ellipsoid plot of **4**. Only the asymmetric unit and Mn coordination sphere have been labeled.

N13–C14–C15 is larger in compensation. There is a weak intramolecular hydrogen bond [S(6); $d_{N2-H2A\cdots Br1A} = 3.427(6)$ Å, $\angle_{N2-H2B\cdots N3A} = 151(6)^\circ$; symm. operation for Br1A $= -x, -y+2, -z+2$], but the pyrimidine ring is not coplanar with the Mn–Br bond [$\angle C_{C2-N1-Mn-Br1A} = 49.4(2)^\circ$].

As with **2** and **3**, the lattice is stabilized by a combination of hydrogen bonding and pi-stacking interactions (Fig. 9). The strong hydrogen bonds between the coordinated and lattice water molecules form rings [$R_4^4(8)$; $d_{O1-H1A\cdots O2B} = 2.734(7)$ Å, $\angle_{O1-H1A\cdots O2B} = 157(6)^\circ$; $d_{O1-H1B\cdots O2C} = 2.743(7)$ Å, $\angle_{O1-H1B\cdots O2C} = 164(8)^\circ$; symm. operation for O2B $= x, y+1, z$; for O2C $= -x+1, -y+1, -z+2$] and between the lattice water molecule and the uncoordinated ring-nitrogen atom [$d_{O2-H3A\cdots N3D} =$ 2.770(7) Å, $\angle_{O2-H3A\cdots N3D} = 169(8)^\circ$] which, with a hydrogen bond between the amino group and the bromine atom, generates a second ring structure [$R_3^3(8)$].

Molecules of **4** are linked into chains parallel to the (100) face diagonal by π-stacking interactions (Fig. 10). The distance between the pyrimidine ring planes is 3.40(1) Å. Successive ring centroids are 3.695(6) Å apart and the angle between the line connecting those centroids and the mean ring plane is 22.8(4)°.

Compound **5** is best described as a co-crystal of $MnBr_2(H_2O)_4$ and (2-apmH_2)Br_2 (Fig. 11). The tetraaquadibromomanganese molecule is nearly octahedral in geometry. The Br1–Mn–Br1A angle is opened slightly [91.22(9)°]. The *cis* O–Mn–O angles are slightly compressed, as is the O2–Mn–O3 angle [170.2(4)°]. The Mn–Br1 bond

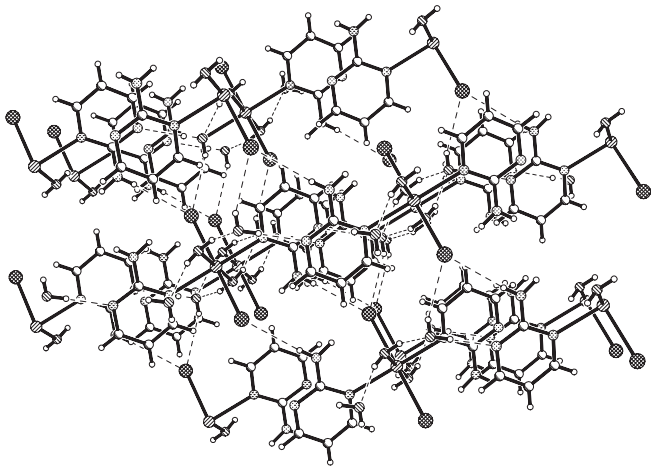

FIGURE 9 Packing diagram of **4** viewed parallel to the *a*-axis, showing hydrogen bonds as dashed lines.

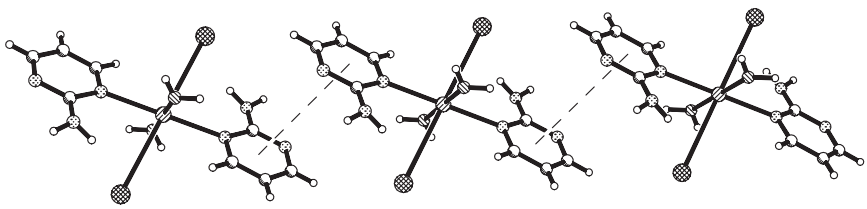

FIGURE 10 Packing diagram showing the π-stacking to form chains in **4**.

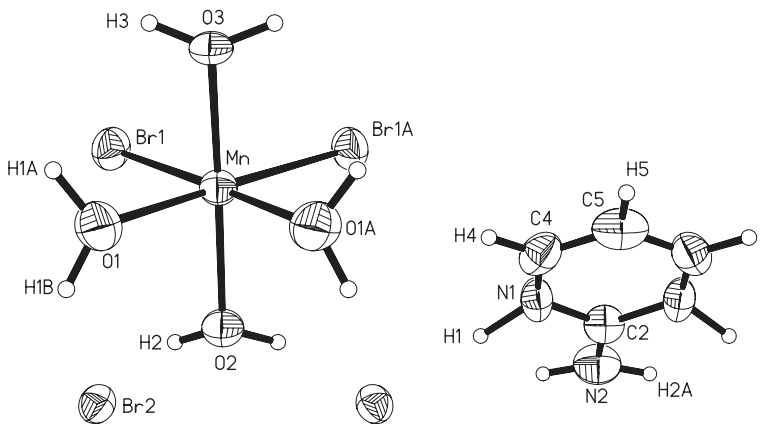

FIGURE 11 Thermal ellipsoid plot of the molecular unit of **5**. Only the asymmetric unit and Mn coordination sphere are labeled. Hydrogen atoms are shown as arbitrary spheres.

[2.655(12) Å] is slightly shorter than in **4** (by ~0.05 Å) while the Mn–O bonds [2.193(8)–2.210(9) Å] are longer by the same amount. Only one reported structure has a neutral $MnBr_2O_4$ core. The $MnBr_2$ complex with 4-hydroxy-4-methyl-2-pentanone has even shorter Mn–Br bonds (2.587 Å) [16] while the Mn–O bonds are longer (Mn–O=C = 2.221 Å, Mn–OH = 2.236 Å).

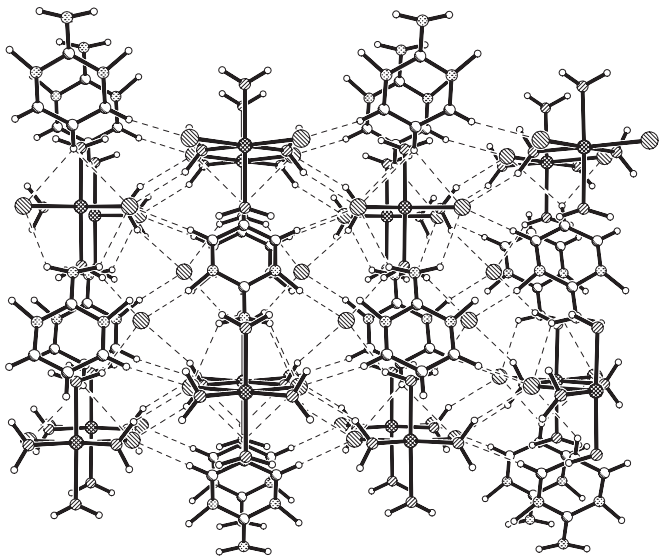

FIGURE 12 Packing diagram of **5** viewed parallel to the *c*-axis (*b* is horizontal). Dashed lines represent hydrogen bonds.

Angular distortion is much more pronounced in the pentanone complex where the Br–Mn–Br angle is 99.4° as a result of the bite angle of the chelating hydroxyketone (76.3°). The coordination polymer *cis*-$MnBr_2(H_2O)_2$(glycine) [17] shows Mn–Br and Mn–OH_2 bond lengths that are similar to the current complexes while the monomeric complex bis(2-pyrrolidinecarboxylic acid)$(H_2O)_2MnBr_2$ [18] has longer Mn–Br bonds (2.747 Å) and shorter Mn–OH_2 bonds (2.178 Å). The latter complex has bond angles closer to the idealized 90°, while the former has a compressed H_2O–Mn–OH_2 bond angle (80.6°).

The C–N bonds within the 2-apmH_2 dication are all equal [1.338(14) Å], as are the C–C bonds within experimental error [1.345(13) Å]. The bond angles at the ring-nitrogen atoms have expanded [122.3(9)°] but the interior angle at C2 is compressed [117.1(13)°].

The complex packs into stacks parallel to the *c*-axis (Fig. 12). The stacks of $MnBr_2(H_2O)_4$ molecules and 2-ampH_2 ions are interweaved so that successive species in a stack are well separated. For example, the ring centroids for 2-apmH_2 ions are 6.985 Å apart, precluding any π-stacking interactions.

The structure is stabilized by an extensive hydrogen-bonding network (Fig. 13 and Table III). The Br1 atoms in a $MnBr_2(H_2O)_4$ molecule are chelated by H-bonding to the NH_2-group[$R_2^2(6)$], and are also H-bonded to O1 of an adjacent $MnBr_2(H_2O)_4$ parallel to the *b*-axis [$C_2^2(8)$, not shown]. The Br2 ions link $MnBr_2(H_2O)_4$ molecules through hydrogen bonds to both the O2 and O3 water molecules [$R_2^2(8)$]. Two additional H-bonds link Br2 ions to the pyrimidinium N (N1) and the O1 water molecule [$R_2^2(12)$, not shown].

Magnetic Susceptibility

The magnetic susceptibility of each sample was measured at room temperature. The molar susceptibilities and Curie constants are: **1**, $\chi_m = 1.55 \times 10^{-2}$ cgs, $C = 4.5$;

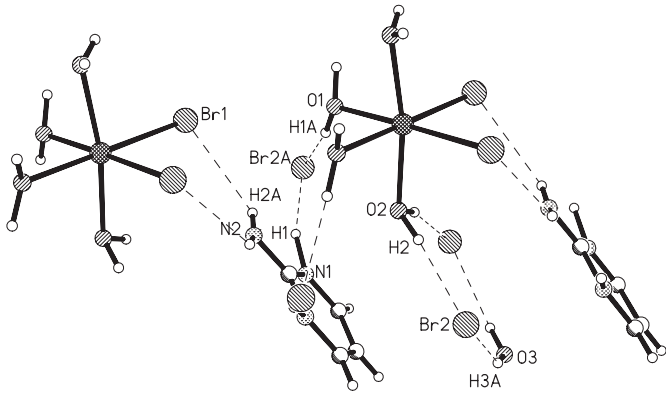

FIGURE 13 Hydrogen bonding in compound **5**.

2, $\chi_m = 1.60 \times 10^{-2}$, $C = 4.6$; **4**, $\chi_m = 1.48 \times 10^{-2}$ cgs, $C = 4.4$; **5**, $\chi_m = 1.46 \times 10^{-2}$ cgs, $C = 4.3$. The expected Curie constant for the isotropic Mn(II) ion is 4.4, showing good agreement with all compounds.

Infrared Spectra

All complexes show absorptions in the 3500–3000 range due to N–H and, for hydrated complexes, O–H stretching vibrations. These are especially pronounced in **4** and **5** due to the high number of water molecules per formula unit. The H–N–H scissoring motion (1650 cm^{-1} in the free ligand [19]) moves to higher energy in the pyrimidinium complexes (compounds **2**, **3** and **5**), and moves to slightly lower energy in the neutral complexes **1** and **4**. The strong ring-absorptions in the 1470–1600 cm^{-1} range also do not shift significantly in the neutral compounds. The out-of-plane H-bending vibration near 785 cm^{-1} varies over ± 10 cm^{-1}, but its position does not correlate with protonation of the ring.

Discussion

The structure of the ligand salt, **3**, is surprising by the absence of dimer formation due to hydrogen bonding [$R_2^2(8)$]. This structural motif (Fig. 14) is perhaps the most common feature in compounds of 2-aminopyrimidine and is seen in the neutral parent compound [20] as well as metal complexes of the neutral ligand such as $[Cu(OMe)(2\text{-apm})]_2(BF_4)_2$ and $[Cu(OMe)(2\text{-apm})]_2(ClO_4)_2$ [21], $CuBr_2(2\text{-apm})_2$ [6], and $[Co(N(CN)_2)_2(2\text{-apm}]_n$ [22]. This dimeric structure is also common in the 2-aminopyrimidinium ion in complexes such as $(2\text{-apmH})_2[Cu_2Br_6]$ [6] and $(2\text{-apmH})_2[Cu_2Cl_6]$ [7a], and 2-aminopyridinium salts such as those with 2,4,6-trinitrobenzoic acid [23] and squaric acid [24]. Instead of the more common dimer formation, **3** develops a chain-like structure parallel to the *b*-axis via consecutive hydrogen bonds from the amino group to the unprotonated ring-nitrogen atom (Fig. 6). These chains are then further linked into sheets via a head-to-tail π-stacking interaction (Fig. 7) where the amino substituents of one ring are centered under the next ring in the chain. This mode of π-stacking is also observed in the 2-aminopyrimidinium fumarate salt [25] and $(2\text{-apmH})_2[Cu_2Cl_6]$ [7a] and also occurs to form simple head-to-tail dimeric structures [26].

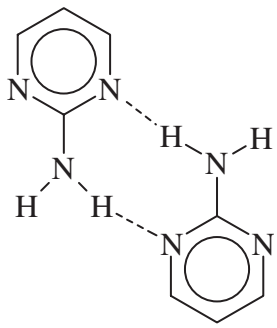

FIGURE 14 Dimerization of 2-aminopyrimidine via hydrogen bonding.

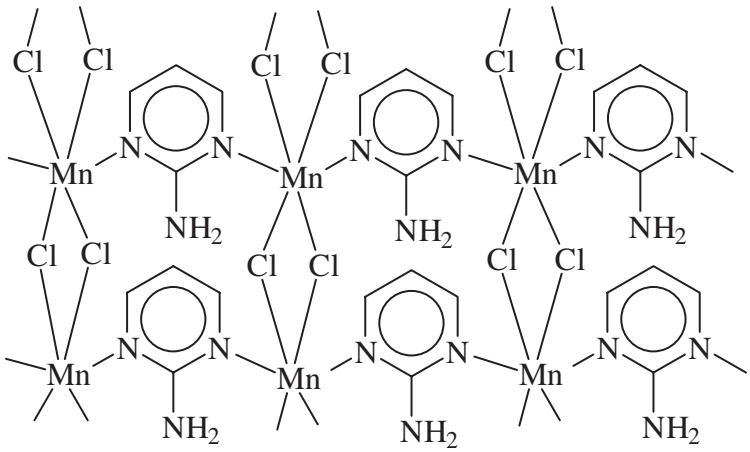

FIGURE 15 Proposed structure of compound **1**.

Although we were unable to grow single crystals suitable for study, we propose that **1** is a two-dimensional coordination polymer, bi-bridged in one direction by chloride ions and linked in the perpendicular direction by bridging 2-apm ligands (Fig. 15). The composition of the material was confirmed by combustion analysis and the molecular weight by room temperature magnetic susceptibility. There is a precedent for such structures in the literature as the copper chloride complex has been reported [2a]. Complexes containing just the bridging 2-amp ligand [6, 27] are well known, as are complexes with the bi-bridged halide linear chain motif with ancillary phosphines [28], amines [29] and water [30]. The χT for **1** indicates that magnetic exchange through the pyrimidine and halogen bridges must be weak.

Under acidic conditions, the dimer structure, **2**, is formed. Extension of the dimers into a ladder motif occurs via hydrogen bonding. Again, there is a good precedent for such a supramolecular motif. In both pyridinium $[Mn(H_2O)Cl_3]$ and quinolium $[Mn(H_2O)Cl_3]$ [31], extended bichloride bridged chains of Mn(II) ions form with a chloride and one water molecule completing the Mn coordination sphere. These chains are then linked into sheets by hydrogen bonds between the axial water molecules in one chain and the axial chloride ion in the next in the same fashion as the dimers of **2**

are linked by hydrogen bonding to form ladders. The ladders are well isolated from each other by the 2-apmH ions that occur as π-stacked tetramers (Figs. 3 and 4). Each stack of four 2-apmH rings terminates into another tetramer stack at right angles, generating a rectangular cavity that surrounds the ladders. Additional supramolecular structure via dimerization of the unprotonated ring-nitrogen is precluded by the strong hydrogen bond between N11 and a coordinated water molecule, linking the π-stacked tetramers to the Mn dimers. As with **1**, χT for **2** agrees with that expected for an isolated Mn(II) ion, indicating weak interactions through the halogen bridge.

Compound **4**, $Mn(2\text{-apm})_2(H_2O)_2Br_2$, is distinct from its Cu(II) [2a], Ni(II) [1] and Co(II) [1] analogs as a result of the coordinated water molecules. This eliminates the semi-coordinate M–X bonds that link the Cu, Ni and Co complexes into chains. Instead, **4** forms chains via π-stacking interactions (Fig. 10) that are further linked into layers parallel to the (010) face via weak hydrogen bonds between the bromide ions of one chain and the amino substituents of the next. Additional hydrogen bonds between the coordinated and lattice waters further link the layers into a three-dimensional lattice.

The $MnBr_2(H_2O)_2$ coordination sphere is unusual. Only two other structures have been reported containing that fragment, and both are complexes with carboxylates. One is a coordination polymer formed by a bridging carboxylate from the glycine zwitterions [17] while the other is the bis-proline complex [18].

The tetraaquadibromomanganese(II) moiety in **5** is even more unusual. The structure of the triaquatribromomanganese(II) ion has been reported as its triethylenediammonium salt [32]. The tetraaquamanganese(II) fragment is well known with its octahedral coordination sphere filled by carboxylates [33], amines [34] and cyanides [35] in both *cis* and *trans* geometries. The diprotonated 2-apmH_2^{2+} ion has been observed previously and the structures of the $CuBr_4^{2-}$ [6] and $CoBr_4^{2-}$ [1] salts have been reported. The isomorphous compound (2-apmH_2)$NiBr_2(H_2O)_4(Br)_2$ has also been reported [1] and shows the same bond lengths and angles, allowing for the expected increase for Mn–Br and Mn–O bonds relative to Ni(II).

The hydrogen-bonding network in **5** is extensive and links the columns of 2-apmH_2^{2+} ions and $Mn(H_2O)_4Br_2$ molecules into an extended three-dimensional network (Figs. 12 and 13). 2-ApmH_2^{2+}/$Mn(H_2O)_4Br_2$ pairs are generated by the chelating H-bonds between NH_2 and $MnBr_2$ moieties. These pairs are then linked into chains parallel to the *b*-axis by hydrogen bonds between the pyrimidinium N–Hs and the ionic bromides. Those chains are then linked into sheets parallel to the (100) face by hydrogen bonds between the ionic bromides and one of the coordinated water molecules (O1). Finally, hydrogen-bond bridges parallel to the *a*-axis between the ionic bromides and the remaining coordinated water molecules (O2, O3) complete the network. The interweaving of the 2-apmH_2^{2+} ions and the $Mn(H_2O)_4Br_2$ molecules precludes any π-stacking between the pyrimidine rings.

CONCLUSIONS

The oxophilic nature of the Mn(II) ion results in a high percentage of hydrated complexes. All the Mn complexes isolated are hydrates, except for the proposed structure of **1**. While surprising in light of the other complexes, the anhydrous nature of **1** is well supported by infrared data. The Mn(II) ions are all six-coordinate,

pseudo-octahedral structures whereas the related complexes with Cu(II), Ni(II) and Co(II) exhibit a mix of coordination numbers and geometries. Three of the complexes show significant π-stacking interactions that generate chains. The presence of water molecules in these compounds also has a significant effect on the structural motifs present. As a result of hydrogen bonding to both coordinated and lattice water molecules, none of the complexes show the $[R_2^2(8)]$ dimers commonly found in aminopyrimidine structures. These hydrogen bonds, however, serve the same role of linking the molecules into supramolecular chains, layers and three-dimensional structures. Work is in progress to extend this family of complexes to the Fe(II) and Fe(III) complexes.

References

[1] M.E. Masaki, B.J. Prince and M.M. Turnbull, *J. Coord. Chem.* **55**, 1337 (2002).
[2] (a) For the previous paper in this series see: B.J. Prince, M.M. Turnbull and R.D. Willett, *J. Coord. Chem.* **56**, 441 (2003); (b) B.J. Prince and M.M. Turnbull, *J. Coord. Chem.* **41**, 339 (1997).
[3] G. Smith, J.M. Gentner, D.E. Lynch, K.A. Byriel and C.H.L. Kennard, *Aust. J. Chem.* **48**, 1151 (1995).
[4] G.A. van Albada, M.E. Quirox-Castro, I. Mutikainen, U. Turpeinen and J. Reedijk, *Inorg. Chim. Acta* **298**, 221 (2000).
[5] M.J. Krische, J.-M. Lehn, N. Kyritsakas and J. Fischer, *Helv. Chim. Acta* **81**, 1909 (1998).
[6] G. Pon, R.D. Willett, B.A. Prince, W.T. Robinson and M.M. Turnbull, *Inorg. Chim. Acta* **255**, 325 (1997).
[7] (a) T. Manfredini, G.C. Pellacani, A. Bonamartini-Corradi, L.P. Battaglia, G.G.T. Guarini, J.G. Giusti, G. Pon, R.D. Willett and D.X. West, *Inorg. Chem.* **29**, 2221 (1990); (b) C. Zanchini and R.D. Willett, *Inorg. Chem.* **29**, 3027 (1990).
[8] XSCANS, Version 2.0. (Siemens Analytical X-ray Instruments, Madison, WI, 1993).
[9] G.M. Sheldrick, SHELXTL: v. 5.10, Structure Determination Software Suite (Bruker AXS Inc., Madison, WI, 2001).
[10] SMART: v.5.625, Bruker Molecular Analysis Research Tool (Bruker AXS, Madison, WI, 2001); SAINTPlus: v. 6.22, Data Reduction and Correction Program (Bruker AXS, Madison, WI, 2001).
[11] G.M. Sheldrick, SADABS: v.2.01, An Empirical Absorption Correction Program (Bruker AXS Inc., Madison, WI, 2001).
[12] G.M. Sheldrick, SHELX97-2. Programs for the Solution and Refinement of Crystal Structures (University of Göttingen, Germany, 1997).
[13] The structures have been deposited with the CCDC. Ref. numbers: **2**, 205802; **3**, 205804; **4**, 205803; **5**, 205805.
[14] M.C. Etter, J.C. MacDonald and J. Bernstein, *Acta Crystallogr., Sect. B* **46**, 256 (1990).
[15] D.M.L. Goodgame, D.A. Grachvogel, S. Holland, N.J. Long, A.J.P. White and D.J. Williams, *J. Chem. Soc., Dalton Trans.* 3473 (1999).
[16] O. Schneider, E. Gerstner, F. Weller and K. Dehnicke, *Z. Anorg. Allg. Chem.* **625**, 1101 (1999).
[17] T. Glowiak and Z. Ciunik, *Bull. Acad. Pol. Sci., Ser. Sci. Chim.* **25**, 277 (1977).
[18] T. Glowiak and Z. Ciunik, *Acta Crystallogr., Sect. B* **33**, 3237 (1977).
[19] (a) M. Maehara, S. Nakama, Y. Nibu, H. Shimada and R. Shimada, *Bull. Chem. Soc. Jpn.* **60**, 2769 (1987); (b) E. Spinner, *J. Chem. Soc.* 3119 (1962).
[20] J. Scheinbeim and E. Schempp, *Acta Crystallogr., Sect. B* **32**, 607 (1976).
[21] H.-L. Zhu, C.-X. Ren and X.-M. Chen, *J. Coord. Chem.* **55**, 667 (2002).
[22] P. Jensen, S.R. Batten, B. Moubaraki and K.S. Murray, *Chem. Commun.* 793 (2000).
[23] K.A. Byriel, C.H.L. Kennard, D.E. Lynch, G. Smith and J.G. Thompson, *Aust. J. Chem.* **45**, 969 (1992).
[24] V. Bertolasi, P. Gilli, V. Ferretti and G. Gilli, *Acta Crystallogr. Sect. B* **57**, 591 (2001).
[25] S. Goswami, A.K. Mahapatra, G.D. Nigam, K. Chinnakali, H.-K. Fun and I.A. Razak, *Acta Crystallogr. Sect. C* **55**, 583 (1999).
[26] (a) T.V. Laine, M. Polamo and M. Leskela, *Z. Kristallogr.* **211**, 639 (1996); (b) A. Luque, J. Sertucha, L. Lezama, T. Rojo and P. Román, *J. Chem. Soc., Dalton Trans.* 847 (1997).
[27] (a) G. Smith, E.J. O'Reilly, C.H.L Kennard and A.H. White, *J. Chem. Soc., Dalton Trans.* 243 (1995); (b) D.E. Lynch and H.L. Duckhouse, *Acta Crystallogr. Sect. C* **56**, e425 (2000); (c) A.J. Blake, P. Hubberstey and C.L. Sampson, *Acta Crystallogr. Sect. E* **58**, m99 (2002); (d) Q.-H. Jin, X.-L. Xin, X.-Y. Ci and K.-B. Yu, *Acta Crystallogr. Sect. C* **58**, m174 (2002).
[28] (a) B. Beagly, J.C. Briggs, A. Hosseiny, W.E. Hill, T.J. King, C.A. McAuliffe and K. Minten, *Chem. Commun.* 305 (1984); (b) S.M. Godfrey, D.G. Kelly, A.G. Mackie, P.P. MacRory, C.A. McAuliffe, R.G. Pritchard and S.M. Watson, *Chem. Commun.* 1447 (1991).

[29] (a) B.C. Unni Nair, J.E. Sheats, R. Ponteciello, D. Van Engen, V. Petrouleas and G.C. Dismukes, *Inorg. Chem.* **28**, 1582 (1989); (b) W. Zhang, J.R. Jeitler, M.M. Turnbull, C.P. Landee, M. Wei and R.D. Willett, *Inorg. Chim. Acta* **256**, 183 (1997).
[30] R.E. Caputo, R.D. Willett and J.A. Muir, *Acta Crystallogr. Sect. B* **32**, 2639 (1976).
[31] R. Caputo, R.D. Willett and B. Morosin, *J. Phys. Chem.* **69**, 4976 (1978).
[32] M. Feist, S. Troyanov, A. Stiewe, E. Kemnitz and R. Kunze, *Z. Naturforsch., Teil B* **52**, 1094 (1997).
[33] (a) M.P. Gupta and B. Mahanta, *Cryst. Struct. Commun.* **7**, 179 (1978); (b) O.M. Yaghi, G. Li and T.L. Groy, *J. Chem. Soc., Dalton Trans.* 727 (1995); (c) Z. Olejnik and T. Lis, *Acta Crystallogr. Sect. C* **56**, 1310 (2000).
[34] (a) Y.-Q. Zheng and J.-L. Lin, *Z. Kristallogr.-New Cryst. Struct.* **216**, 353 (2001); (b) R. Hauptmann, M. Kondo and S. Kitagawa, *Z. Kristallogr.-New Cryst. Struct.* **215**, 171 (2000); (c) C.S. Hong and Y. Do, *Inorg. Chem.* **37**, 4470 (1998).
[35] (a) B. Zeigler, M. Witzel, M. Schwarten and D. Babel, *Z. Naturforsch., Teil B* **54**, 870 (1999); (b) D. Babel and W. Kurtz, *Stud. Inorg. Chem.* **3**, 593 (1983); (c) R. Lescouezec, F. Llortet, M. Julve, J. Vaissermann and M. Verdeguer, *Inorg. Chem.* **41**, 818 (2002).